RESEARCH ARTICLE

Human Mutation

OFFICIAL JOURNAL

HGVS

HUMAN GENOME
VARIATION SOCIETY
www.hgvs.org

Mutations in *MEF2C* from the 5q14.3q15 Microdeletion Syndrome Region Are a Frequent Cause of Severe Mental Retardation and Diminish *MECP2* and *CDKL5* Expression

Markus Zweier,[1] Anne Gregor,[1] Christiane Zweier,[1] Hartmut Engels,[2] Heinrich Sticht,[3] Eva Wohlleber,[2] Emilia K. Bijlsma,[4] Susan E. Holder,[5] Martin Zenker,[1] Eva Rossier,[6] Ute Grasshoff,[6] Diana S. Johnson,[7] Lisa Robertson,[7] Helen V. Firth,[8] Cornelia Kraus,[1] Arif B. Ekici,[1] André Reis,[1] and Anita Rauch[9]*

[1]Institute of Human Genetics, Friedrich-Alexander-University Erlangen-Nuremberg, Erlangen, Germany; [2]Institute of Human Genetics, Rheinische Friedrich-Wilhelms-University, Bonn, Germany; [3]Institute of Biochemistry, Friedrich-Alexander-University Erlangen-Nuremberg, Erlangen, Germany; [4]Department of Clinical Genetics, Leiden University Medical Centre, Leiden, The Netherlands; [5]North West Thames Regional Genetics Service, North West London Hospitals NHS Trust, Harrow, United Kingdom; [6]Institute of Human Genetics, University of Tuebingen, Tuebingen, Germany; [7]Sheffield Children's Hospital, Western Bank, Sheffield, United Kingdom; [8]Department of Medical Genetics, Addenbrooke's Hospital NHS Trust, Cambridge, United Kingdom; [9]Institute of Medical Genetics, University of Zurich, Zurich-Schwerzenbach, Switzerland

ABSTRACT: The etiology of mental retardation remains elusive in the majority of cases. Microdeletions within chromosomal bands 5q14.3q15 were recently identified as a recurrent cause of severe mental retardation, epilepsy, muscular hypotonia, and variable minor anomalies. By molecular karyotyping we identified two novel 2.4- and 1.5-Mb microdeletions of this region in patients with a similar phenotype. Both deletions contained the *MEF2C* gene, which is located proximally to the previously defined smallest region of overlap. Nevertheless, due to its known role in neurogenesis, we considered *MEF2C* as a phenocritical candidate gene for the 5q14.3q15 microdeletion phenotype. We therefore performed mutational analysis in 362 patients with severe mental retardation and found two truncating and two missense de novo mutations in *MEF2C*, establishing defects in this transcription factor as a novel relatively frequent autosomal dominant cause of severe mental retardation accounting for as much as 1.1% of patients. In these patients we found diminished *MECP2* and *CDKL5* expression in vivo, and transcriptional reporter assays indicated that *MEF2C* mutations diminish synergistic transactivation of E-box promoters including that of *MECP2* and *CDKL5*. We therefore conclude that the phenotypic overlap of patients with *MEF2C* mutations and atypical Rett syndrome is due to the involvement of a common pathway.
Hum Mutat 31:722–733, 2010. © 2010 Wiley-Liss, Inc.

KEY WORDS: mental retardation; MEF2C; MECP2; CDKL5; Rett syndrome; epilepsy

Introduction

The etiological understanding of severe mental retardation in the absence of metabolic disorders, gross malformations, and major dysmorphism is limited. For a long time Angelman syndrome (MIM♯ 105830) caused by defects in the *UBE3A* gene (MIM♯ 601623) and Rett syndrome (MIM♯ 312750) caused by X-linked dominant mutations in the *MECP2* gene (MIM♯ 300005) represented the only relatively frequent diagnoses in such patients. Only recently mutations in *CDKL5* (MIM♯ 300203) [Archer et al., 2006; Weaving et al., 2004] and *FOXG1* (MIM♯ 164874) [Ariani et al., 2008; Mencarelli et al., 2010; Philippe et al., 2010] evolved as important differential diagnoses in patients with atypical Rett syndrome. In addition, mutations in *TCF4* (MIM♯ 602272) causing Pitt-Hopkins syndrome also cause a similar, relatively frequent phenotype [Amiel et al., 2007; Brockschmidt et al., 2007; Zweier et al., 2007a, 2008], and mutations in *SYNGAP1* (MIM♯ 603384) were reported to account for 3% of patients with nonsyndromic severe mental retardation, hypotonia and seizures [Hamdan et al., 2009].

Microdeletions sizing between 3.5 and 17 Mb within chromosomal bands 5q14.3q15 were recently identified in a total of six patients to cause a common phenotype with severe mental retardation, epilepsy, muscular hypotonia, and variable brain and minor other anomalies [Cardoso et al., 2009; Engels et al., 2009]. The smallest region of overlap (SRO) was refined to 1.6 Mb containing the *CETN3*, *AC093510.2*, *POLR3G*, *LYSMD3*, and *GPR98/MASS1* genes [Engels et al., 2009]. Five further patients with variable deletions within 5q14.3q15, including one with deletion of *MEF2C* only, and one patient with a truncating mutation in *MEF2C*, were recently described with a similar phenotype, suggesting haploinsufficiency of *MEF2C* as the underlying cause of the 5q14.3q15 microdeletion syndrome despite its location outside the SRO [Le Meur et al., 2010]. In parallel, we identified two novel de novo deletions within 5q14.3 located proximally adjacent to the formerly published SRO including *MEF2C*, which was recently shown to cause a Rett syndrome-like phenotype in conditional knockout mice [Li et al., 2008a]. We therefore also considered *MEF2C* as a candidate for

the phenocritical gene of the 5q14.3q15 microdeletion syndrome, and assumed that the phenotype in the patients with nonoverlapping deletions was caused by a positional effect. To prove this hypothesis we sequenced the coding region of *MEF2C* in 362 patients with severe mental retardation of unknown etiology and detected four de novo mutations, which we studied further to elucidate the underlying pathomechanism.

Materials and Methods

Patients

Patients with severe mental retardation of unknown etiology were recruited from the genetic clinic when no clinical diagnosis was made and conventional karyotyping by GTG-banding with an average banding resolution of 500 and subtelomeric screening either by FISH or MLPA revealed normal results. These patients included 141 patients with moderate to severe mental retardation and a variety of other signs (group 1), and 221 patients with a severe mental retardation level such as seen in Rett, Angelman, or Pitt-Hopkins syndromes without gross malformations or specific dysmorphism (group 2). Clinical and deletion data from patients 1–3 were previously published [Engels et al., 2009]. Informed consent was obtained from the parents, and the study was approved by the ethical review board of the medical faculty of the Friedrich-Alexander University of Erlangen-Nuremberg.

Molecular Karyotyping

Molecular karyotyping was performed using the high-resolution Genome-Wide Human SNP Array 6.0 (Affymetrix, Santa Clara, CAa) and the Affymetrix Genotyping Console Software (Version 3.0.2) according to the supplier's instructions.

MLPA

MLPA probes for all *MEF2C* exons were designed according to the instructions of MRC-Holland, and the reaction was performed using the SALSA MLPA reagents EK5 (MRC-Holland, Amsterdam, The Netherlands) (Supp. Table S1). Each Probemix contained additionally four internal control probes. Copy number values were calculated using values from four healthy control individuals and the Seqpilot software (JSI Medical Systems, Kippenheim, Germany).

Mutational Screening

All coding exons of *MEF2C* (both isoforms NM_002397.3 and NM_001131005.1) with exon–intron boundaries were amplified by PCR and sequenced using the BigDye Terminator v3.1 Cycle Sequencing RR-100-Kit (Applied Biosystems, Foster City, CA) and an ABI 3730 sequencer (Applied Biosystems). Sequencing for screening purposes was performed unidirectionally. Mutations were confirmed by bidirectional sequencing from an independent polymerase chain reaction (PCR) product. Primer sequences are summarized in Supp. Table S2.

Real-Time RT-PCR

cDNAs were obtained from the Human Fetal Multiple Tissue cDNA (MTC) Panel and from the Human Adult Multiple Tissue cDNA (MTC) Panel (Clontech, Mountain View, CA). Real-time PCR studies were performed using custom designed primers and

probes for *MEF2C* isoforms (*MEF2C* Isoform 1 forward primer AATACGATGCCATCAGTGTCTGA, reverse primer AGCC-GACTGGGAGTTATTTATCC, probe ACCTGCTTTTGAATCAA; *MEF2C* Isoform 2 forward primer TTCCACCAGGCAGCAAGAA, reverse primer AGCCGACTGGGAGTTATTTATCC, probe ATGC-CATCAGTGAATCA). Results of four technical replicates each were normalized to the mean of three endogenous controls (β-2-microglobulin [huB2M], actin beta [huACTB], acidic ribosomal protein [huPO]). Normalized expression levels were set in relation to *MEF2C* isoform 1 in fetal brain.

To measure expression of genes in patients with *MEF2C* deletions or mutations, RNA was extracted using the PAXgene™ Blood System (Becton Dickinson, Heidelberg, Germany) and transcribed reversely using Superscript II (Invitrogen, Carlsbad, CA). Analysis of *MEF2C* was performed using the custom designed assay described above. To measure the expression of *TCF4*, *MECP2*, and *CDKL5* predesigned TaqMan Gene Expression Assays were used (CDKL5: Hs00177340_m1, MECP2A: Hs00172845_m1, MECP2B: Hs01598237_m1, TCF4: Hs00162613_m1; Applied Biosystems). Expression levels were quantified by real-time PCR in four replicates each as previously described [Rauch et al., 2008], and results were normalized to the mean of four endogenous controls (β-2-microglobulin [huB2M], actin beta [huACTB], acidic ribosomal protein [huPO], transcription factor IID [huTBP]). Normalized expression levels were set in relation to 10 controls, or if gender matched in relation to six female and four male controls, respectively.

Constructs and Transcriptional Reporter Assay

To express MEF2C in vitro the coding sequence of *MEF2C* isoform 1 (splice variant 2S [Janson et al., 2001]) was amplified from human cDNA, cloned into a TOPO-TA vector (Invitrogen) and then subcloned via BamHI and XhoI sites into the pcDNA3.1 expression vector (Invitrogen). The mutations (G27A, E34X, L38Q) were inserted according to the instructions of the Quick-Change Site-Directed Mutagenesis Kit (Stratagene, La Jolla, CA) with minor modifications.

For testing of coactivation of E-boxes by wild-type and mutant MEF2C, we used a luciferase reporter construct containing a herpes simplex thymidine kinase promoter, either without binding sites (tkGL2) or with four E boxes (4 × EtkGL2) located within the pTa enhancer, and also containing a T/A rich MADS consensus binding site [(C/T)TAT(T/A)3TA(A/G)] [Shore and Sharrocks, 1995] in the backbone of the vector. These constructs were previously used in a transcriptional reporter assay to study the E-box transcription factor TCF4 [Zweier et al., 2007a].

For the *MECP2*-specific luciferase reporter construct the described *MECP2* promoter (−1,071 until +9 bp) [Liu and Francke 2006] region was amplified from normal human DNA, cloned into a Topo TA vector, and then subcloned into the pGL3 vector (Promega, Madison, WI) via SacI and XhoI restriction sites. This *MECP2* promoter contains 10 E-box motives but no MADS binding site.

For the *CDKL5*-specific luciferase reporter construct a ~1.2 kb genomic fragment, located 81.1 kb to 82.3 kb proximal of the start codon of *CDKL5* isoform I (NM_003159.2) and containing the untranslated exon 1, was amplified from normal human DNA, cloned into a Topo TA vector, and then subcloned into the pGL3 vector (Promega) via SacI and NheI restriction sites. This *CDKL5* promoter contains three E-box motives but no MADS binding site.

All above-mentioned constructs were sequence verified. For all three reporter assays JEG3 cells were cultivated in RPMI medium

containing 10% FCS and then transiently cotransfected, using PLUS reagent and Lipofectamine 2000 (Invitrogen) with 100 ng of the *MEF2C* wild-type or mutant constructs, 1 µg of one of the reporter constructs (4 × EtkGL2, *MECP2* promoter in pGL3, *CDKL5* promoter in pGL3) or the respective negative control (tkGL2, pGL3) and a renilla luciferase vector (25 ng) used for normalization to exclude differences in transfection efficiency. Cells were harvested 48 h after transfection and luminescence measurements were performed with a Dual Luciferase Kit (Promega) and a luminometer. Each experiment was performed in triplicate and confirmed by a second, independent triplicate experiment. Depicted datapoints in the diagrams represent the mean and the standard deviation of three independent transfections from one experiment. The *P*-values were calculated using the Student *t*-test on the total of six values from the two independent sets of experiments.

We showed previously, that a similar assay using t-boxes did not work with the developmental transcription factor *TBX1* in HEK293 cells, but in JEG3 cells, which are derived from human chorioncarcinoma [Zweier et al., 2007b]. Assuming, therefore, that JEG3 cells would contain a transcriptional factor profile suitable to study developmental genes, we used this JEG3 cells also to analyze MEF2C.

Homology Modeling

The effects of the mutations on the MEF2C structure were assessed on the basis of the high-resolution crystal structure of the DNA binding domain of MEF2A in complex with DNA (PDB code 1egw) [Santelli and Richmond 2000]. Apart from a conservative serine to threonine replacement at position 51, MEF2A and MEF2C exhibit an identical sequence in the respective protein domain. Mutations within MEF2C were generated using Sybyl7.3 (Tripos Inc., St. Louis, MO) and the effect of the mutations was assessed using the programs Procheck [Laskowski et al., 1993] and WhatCheck [Hooft et al., 1996].

Results

By molecular karyotyping we identified a novel 2.4 Mb de novo deletion within 5q14.3 in a 2-year-old girl (P4) with severe psychomotor retardation, hypotonia, seizures, and minor anomalies (Table 1, Fig. 1A, and Fig. 2E–H). The first and last deleted probes as indicated by the array were CN_1148990 (hg18: chr5:85,676,966) and CN_1126764 (hg18: chr5: 88,097,879) [g.(85,447,085_85,676,966)_(88,097,879_88,099,696)del NCBI Build 36.1]. By MLPA the deletion was confirmed to include exons 5–11 of *MEF2C* in the patient and to be absent in both parents. One further patient with a similar phenotype (P9) was found to harbor an 1.5-Mb deletion spanning *MEF2C* and two further genes (Table 1, Fig. 1A, and Fig. 2I and J). The deletion of this patient was excluded in the mother, but the father was not available. The first and last deleted probes as indicated by the array were CN_1124402 (hg18: chr5: 87,400,499) and CN_1133344 (hg18: chr5: 88,895,460) [g.(87,397,069_87,400,499)_(88,895,460_88,896,692)del NCBI Build 36.1]. Deletion of *MEF2C* was excluded by MLPA with probes for each exon of isoform 1 in patient P3, whom we reported previously to harbor a 5q14.3q15 microdeletion [Engels et al., 2009]. By sequencing the coding region of *MEF2C* in 362 patients with severe mental retardation of unknown etiology we detected four de novo mutations, all in patients from group 2 (P5–8; Table 1, Fig. 1B, and Fig. 2K–T). Expression studies of *MEF2C* isoforms by quantitative RT-PCR in

various human fetal and adult tissues showed that isoform 1 was detectable only in high levels in brain, whereas isoform 2 was widely expressed with highest level in skeletal muscle (Fig. 3). Homology modeling of the two *MEF2C* missense mutations predicted that both mutations lead to steric clashes with nearby side chains, thus most likely affecting specificity of DNA binding (Fig. 4). Analyses of relative expression levels of *MEF2C* isoform 2 and potentially related genes in patients RNA derived from blood revealed significantly decreased *MEF2C* expression in all patients with deletions in the region of *MEF2C* as well as in patients with *MEF2C* truncating mutations, but not in the two patients with missense mutations (P5 and P8). Of note, P3, in whom the deletion ends 5′ of *MEF2C* also showed a significantly diminished *MEF2C* expression level (Fig. 5). *MECP2* expression of both isoforms was significantly decreased in all patients compared to gender matched controls, and *CDKL5* was significantly decreased in the majority of patients but not in P4 and P9 with *MEF2C* deletions. Expression of *TCF4* was not consistently altered in patients with *MEF2C* deletions or mutations.

Results of transcriptional reporter assays using either a MADS-box and an E-box enhancer element with a tk promoter, the E-box containing *MECP2* or *CDKL5* promoters are shown in Figure 6. In all three assays wild-type MEF2C showed significant transcriptional activity, which was consistently abolished by stop and missense mutants.

Cotransfection of 4 × EtkGL2 containg E-boxes and a MADS-box with *MEF2C* wild type significantly increased the transactivation of the reporter construct reaching 6.5-fold values compared to cotransfection of 4 × EtkGL2 with an empty CMV vector. For all three mutant *MEF2C* constructs E34X, L38Q, and G27A transactivation of the reporter construct was significantly decreased, with the G27A mutation showing the mildest effect and the E34X mutation showing the strongest effect (Fig. 6A).

Transfection of the reporter construct containing the *MECP2* promoter with an empty CMV expression vector alone resulted in an 800-fold increased activation of the luciferase gene compared to the empty luciferase vector pGL3 (Fig. 6B). Cotransfection of *MEF2C* showed a significant further increase of the promoter activation. All *MEF2C* mutants significantly diminished the activity of the *MECP2* promoter back to the level of the *MECP2* promoter alone.

Similar effects of promoter activity were observed for the reporter construct containing the *CDKL5* promoter region (Fig. 6C), which resulted in an 70-fold activation of the luciferase gene compared to the empty pGL3 vector. Cotransfection of wild-type *MEF2C* also significantly further increased transcriptional activity, which was again abrogated by the mutations.

Discussion

We identified two patients with novel deletions within 5q14.3 (P4, P9) who resemble patients with the recently defined 5q14.3q15 microdeletion syndrome, although they do not share deletion of any gene from the reported smallest region of overlap [Engels et al., 2009]. Both of these novel deletions in our patients included *MEF2C*, which was recently shown to cause a Rett syndrome-like phenotype in conditional null mice [Li et al., 2008a]. We therefore considered *MEF2C* as a candidate for the phenocritical gene of the 5q14.3q15 microdeletion syndrome, and assumed that the phenotype in the patients with nonoverlapping deletions was caused by a positional effect. To prove this hypothesis, we analyzed *MEF2C* expression by quantitative real-time PCR in RNA derived from blood of patients P1–P9,

Table 1. Summary of Clinical Features in Patients with 5q14.3q15 Microdeletions and *MEF2C* Point Mutations

| | Previously described by Engels et al. [2009] | | | | P5 | P6 | P7 | P8 | P9 | 3 patients from Cardoso et al. [2009] | C7 from Le Meur et al. [2009] | Patients C1-5 from Le Meur et al. [2009] |
	P1	P2	P3	P4								
Genetic defect	5.7 Mb deletion including *MEF2C*	3.8 Mb deletion including *MEF2C*	3.6 Mb deletion 5q14.3q15	2.4 Mb deletion including exons 5–11 of *MEF2C*	*MEF2C* c.113T>A, p.L38Q	*MEF2C* c.99dupT, p.E34X	*MEF2C* c.226_236del11, p.H76fsX15	*MEF2C* c.80G>C, p.G27A	1.5 Mb deletion including *MEF2C*	microdeletions 5q14.3q15 (patient 2 including *MEF2C*)	*MEF2C* c.683C>G, p.S228X	microdeletions 5q14.3q15 from 216 kb to 8.8 Mb, all including *MEF2C*
Age at last investigation	6y	8y	6y7mo	2y2mo	3y	14y	7y	10y5mo	3y	7y, 5y, 5y	7y	4y9mo, 9mo, 1y6mo, 3y, 8y
Gender	female	female	female	female	female	male	female	female	male	male, female, male	female	female, female, male, male, female
Height	P10	P9	P10	P75–P90	n. k.	P10	P5	P25–50	P25	n. k., n. k., n. k.	P50	P25–50, P25–50, P50, P75–90, P10–25
Weight	n. k.	P2–P9	P25	P10–P25	P25	P3	<P2	P50	<P3	n. k., n. k., n. k.	P50	P25–50, >P97, <P3, P10–25
Head circumference	P90–97	P2–P9	P10–P25	P50	P9	P3	P50	P50	P10–25	n. k., n. k., >P98	>P97	P25–50, <P3, P75–90, P25–50, P3–10
Severe MR	+	+	+	+	+	+	+	+	+	+, +, +	+	+, +, +, +, +
Regression	−	−	−	−	−	−	−	−	−	−, −, −	+ (5mo)	−, −, −, −, −
Autistic features	−	−	−	+	+	+	−	n. k.	(+)	−, −, +	poor eye contact	C1-5 poor eye contact
Hypotonia	+	+	+	+	+	hypertonia	+	+	+	+, −, +	−	+, +, +, +
Seizures, first at age	1d	febrile during infancy	4y5mo	febrile at 1y	10mo	complex partial, 10mo	3–6mo	6mo	spasms, myoclonic events 3mo	1y, 9mo, 8mo	9mo	4mo, neonatal, −, −, 3y
Stereotypic hand movements	−	−	+	−	−	−	−	−	+	n.n, n.n., n.n.	+	+, −, −, +, +
Strabism	+	−	+	+	+		+	+	(+)	+, −, −	+	−, −, −, −
MRI anomalies	+	+	+	mildly enlarged extracerebral CSF space, two unspecific white matter lesions in the internal capsule/insular and the parieto-dorsal regions	generalized lack of white matter bulk and delay in myelin maturation	mildly enlarged ventricles	−	mild under myelinisation of insular cortices bilaterally	mild under myelinisation	P1-P3 periventricular heterotopias; P3 polymicrogyria, under rotated hippocampi	enlarged lateral ventricles, periventricular white-matter hyperintensities	C1 frontoparietal atrophy, enlarged pericerebral spaces; C2 enlarged lateral ventricles, reduced cortical gyration; C3 verticalisation of the tent of the cerebellum, enlarged 4th ventricle; C4 enlarged 4th ventricle; C5-
Breathing anomalies	−	−	−	−	−	−	−	episodic hyperventilation	−	−, −, −	−	C5 episodic hyperventilation and apnea
Walking (age)	−	−	−	−	−	2y8mo	−	with support (8y)	−	5y, −, 3y	3y	−, −, −, −, −
Speech	−	−	−	−	−	−	−	−	−	−, −, −	−	−, −, −, −, −
Large ears	+	−	+	+	+	(+)	−	(+)	+	−, −, −	+	+, +, +, +, +

TABLE 1. Continued

	Previously described by Engels et al. [2009]				P5	P6	P7	P8	P9	3 patients from Cardoso et al. [2009]	C7 from Le Meur et al. [2009]	Patients C1-5 from Le Meur et al. [2009]
	P1	P2	P3	P4								
Broad forehead	−	−	+	+	+	+	+	+	+	+, +, +	+	+, +, +, +, +
Prominent ear lobe	+	n.n.	+	+	+	(+)	+	fleshy	+	n. n., n., n., n. n.	+	+, +, +, −, −
Upslanting palpebral fissures	mild	−	mild	mild	mild	mild	−	downslanting	−	downslanting, −, −	−	+, +, −, −, −
Widely spaced teeth	−	n.n.	n.n.	+	+	−	+	− crowded	−	n. n., n. n., n. n.	n. k.	n. k., n. k., n. k., +, +
Upper lip anomalies	cupid bowed	−	cupid bowed	cupid bowed tented	cupid bowed	tented in infancy, cupid bowed	tented	full	slightly cupid bowed	P1–P2 flat long philtrum, P2 thin lips, −	downturned corners	C1 tented, C2 tented, C3 flat philtrum, C4 flat philtrum, C5 short philtrum
Others			hyper-metropia	sleeping problems, dystonia	high glycine in urine	hypermetropia, normal puberty, needs feeding, daytime continence	heterochromasia, high pain tresh-hold, sleeping problems, joint hyperlaxity	nails grow quickly, thick hair	nystagmus,	P1 iris coloboma, high arched eyebrows, flat nasal bridge, thick columella, and hypertelorism; P2 frontal bossing, hypertelorism, anteverted nostrils, high arched eyebrows, depressed nasal bridge, thick columella, micrognathia; P3 postaxial polydactyly of right toes	feeding difficulties	C2 oedema of hands and feet; C3 bilateral 2–3 toe syndactyly, ectois testis, cortical blindness, sleep disturbance; C4 left 2–3 toe syndactyly, agenesis of right toes 2–5 distal phalange; C5 parents first cousins
Normal diagnostic Pretesting				AS	AS	AS	TCF4	AS	ARX	P1–P3 FLNA	MECP2	C1 CDKL5
					MECP2 TCF4		MECP2 CDKL5 UBE3A 317K SNP array (Illumina) DMPK	TCF4	CDLK5 SLC2A1		CDKL5	C4 AS C5 MECP2
Normal testing after knowledge of expression data	MECP2		MECP2	MECP2	CDKL5	MECP2		MECP2	MECP2			
	CDKL5		CDKL5	CDKL5	CDKL5	CDKL5		CDKL5				

(+) Presence of feature in a mild degree; n.k., not known; n.n., not noticed; AS, genetic testing for Angelman syndrome; SD, standard deviation score; d, days; mo, months; y, years; facial dysmorphism of the patients published by Le Meur et al. [2009] were reevaluated from the published photographs. Nucleotide numbering reflects cDNA numbering with +1 corresponding to the A of the ATG translation initiation codon in the reference sequence (GenBank NM_002397.3), according to journal guidelines (www.hgvs.org/mutnomen). The initiation codon is codon 1.
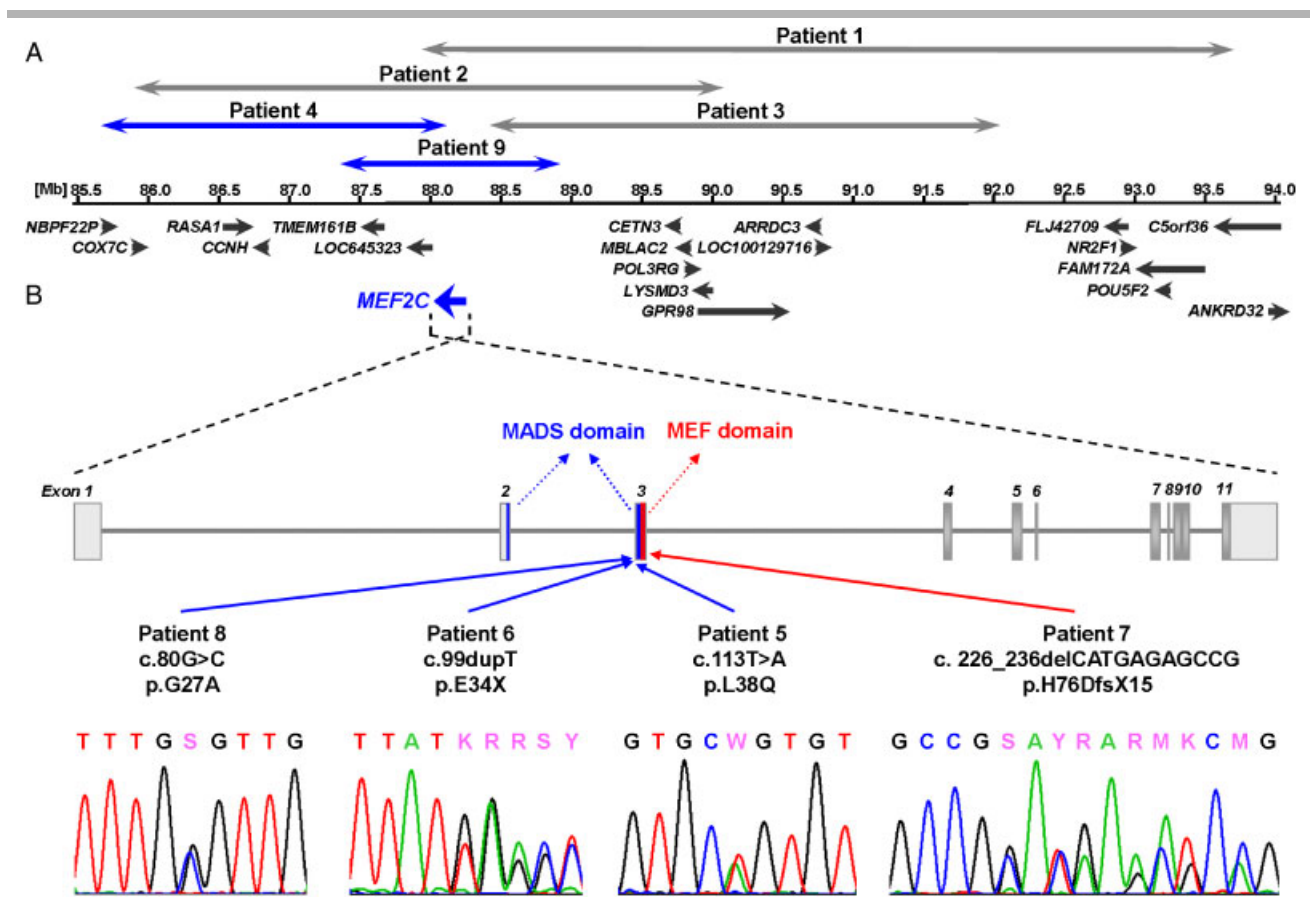
Figure 1. *MEF2C* deletions and mutations. **A:** Schematic drawing of the genomic region 5q14.3q15 with the location of the deletions of our two novel patients (blue arrows) and three published patients [Engels et al., 2009] (gray arrows). Genes represent RefSeq genes from the UCSC genome browser (hg18). **B:** Schematic drawing of exon–intron structure of *MEF2C* isoform 1 with electropherograms and localization of mutations in patients 5–8. Noncoding exons are shown in light gray, exons coding for the MADS domain in blue, and the coding region for the MEF domain is depicted in red. Nucleotide numbering reflects cDNA numbering with +1 corresponding to the A of the ATG translation initiation codon in the reference sequence (GenBank NM_002397.3), according to journal guidelines (www.hgvs.org/mutnomen). The initiation codon is codon 1.

including the previously published patient 3, in whom *MEF2C* was not deleted. Because isoform 1 was not expressed in blood, we analyzed expression of isoform 2 and found significantly reduced *MEF2C* mRNA levels in all patients with either a microdeletion or a truncating mutation (P1–P4, P6–P7, P9). Because the deletion of P3 was reported to start only 329 kb upstream of the start codon of *MEF2C* we confirmed normal genomic dosage for all coding *MEF2C* exons by MLPA, indicating a regulatory positional effect on *MEF2C* expression as the underlying mechanism in this patient. Because *MEF2C* thus apparently represented the only commonly affected gene, we considered *MEF2C* as the critical gene underlying the 5q14.3q15 microdeletion syndrome. We therefore sequenced the coding region of *MEF2C* in 362 patients with severe mental retardation of unknown etiology and detected four de novo mutations (P5–P8). Our finding is in line with the recent report of a patient with a deletion encompassing the *MEF2C* gene only, and a further patient with a *MEF2C* truncating mutation [Le Meur et al., 2010].

The phenotype of the patients with *MEF2C* point mutations was similar to that of patients with microdeletions encompassing further genes and consistently included head circumference within the normal range, severe mental retardation with absence of speech and limited ability to walk freely, seizure disorders with onset in infancy and a common, but not easily recognizable facial gestalt including broad, high forehead, relatively large, backward rotated ears with prominent ear lobes, mildly upward-slanting palpebral fissures, and cupid bowed or tented upper lip (Fig. 2 and Table 1). Most patients showed severe hypotonia and variable subtle brain anomalies in MRI scans, but the periventricular heterotopia described by Cardoso et al. [2009] was neither observed in our patients nor in the patients reported by Le Meur et al. [2010]. Because periventricular heterotopias have been shown to occasionally occur in many different microdeletion syndromes, this feature may be considered an unspecific finding in developmental mental disorders [van Kogelenberg et al., 2010].

MEF2C belongs to the myocyte enhancer factor 2 (MEF2) subfamily of the MADS (MCM1-agamous-deficiens-serum response factor) gene family of transcription factors. The MEF2 transcription factors are characterized by a highly conserved N-terminal MADS-box and an immediately adjacent MEF2 domain motif, which together mediate dimerization, DNA binding, and cofactor interactions. Their transcriptional activity relies on the recruitment of, and cooperation with, many other transcription factors, as well as on translational and posttranslational modifications [Potthoff and Olson 2007]. Although vertebrates have four MEF2 genes, *MEF2A-D*, yeast, *Drosophila,* and *Caenorhabditis elegans* possess only a single *Mef2* gene. There is increasing evidence for a

Figure 2. Facial appearances of patients with *MEF2C* deletions and mutations. **A–J:** Patients with *MEF2C* microdeletions. Patient 1 at the age of 6 (**A**) and 14 years (**B, C**), patient 3 at the age of 6.5 years (**D**), patient 4 at the age of 2 months (**E, F**) and at the age of 2 years 2 months (**G, H**), patient 9 at the age of 3 years (**I, J**). **K–T:** Patients with *MEF2C* mutations. Patient 7 at the age of 2 (**K**) and 5 years (**L**), patient 5 at the age of 2 years 4 months (**M**) and 3 years (**N**), patient 8 at the age of 10.5 years (**O, P**), patient 6 at the age of 3 (**Q, R**) and 14 years (**S, T**).

pivotal role of Mef2c in myogenesis, the development of the anterior heart field, neural crest and craniofacial development, chondrocyte hypertrophy and vascularization, endothelial cell proliferation and survival, lymphoid development, neurogenesis, and synaptic formation [Li et al., 2008a, 2008b; Potthoff and Olson 2007; Stehling-Sun et al., 2009]. The four vertebrate *Mef2* genes display overlapping, but distinct temporal and spatial expression patterns during embryonic development and in adult tissues, with highest expression in striated muscles and brain [Edmondson et al., 1994]. *Mef2c* was found to be highly expressed in the embryonic cerebral cortex, hippocampus, amygdala, midbrain, olfactory bulb, and cerebellum, as well as in the adult frontal cortex, dentate gyrus, hippocampus, thalamus, and cerebellum [Lyons et al., 1995]. Notably, a *MEF2C* isoform was cloned from human cDNA that was expressed in the brain but not in muscle [Leifer et al., 1993]. To analyze the expression pattern of the two human RefSeq *MEF2C* isoforms we performed quantitative real-time PCR for each isoform in a panel of human tissues. We found expression of *MEF2C* isoform 1 (NM_002397.3), which shares the MADS and MEF2 box regions with isoform 2 (NM_001131005.1), to be restricted in high levels to fetal and
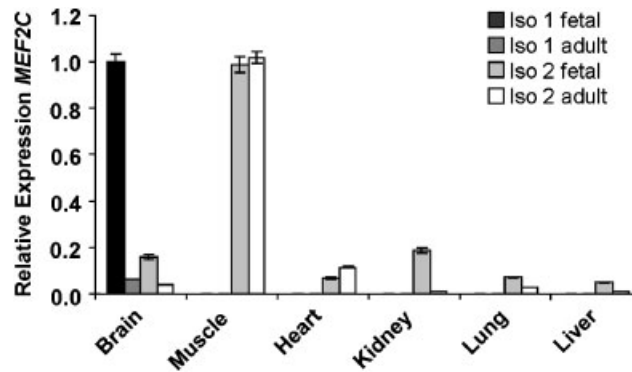

Figure 3. Expression of the two different isoforms of *MEF2C* in several human tissues, measured by quantitative real-time RT-PCR analysis. Isoform 1 is shown in black (fetal tissues) and dark gray (adult tissues), isoform 2 in light gray (fetal tissues) and white (adult tissues). The values were obtained in four replicates, normalized to three different housekeeping genes and set in relation to isoform 1 in fetal brain. The diagram shows the mean values with standard deviation for each tissue. Isoform 1 showed detectable expression in high levels only in brain, whereas isoform 2 was widely expressed with highest level in skeletal muscle.

adult brain, whereas isoform 2 was detected in all tissues tested, with highest expression in skeletal muscle (Fig. 3).

Two of the four mutations detected in our patients introduced a premature stop codon while both missense mutations changed the MADS domain and were assumed to alter DNA-binding affinity by means of homology modeling (Fig. 4). To prove that *MEF2C* is indeed haploinsufficient in patients with *MEF2C* mutations, we analyzed *MEF2C* expression by quantitative real-time PCR in RNA derived from blood, and as in patients with deletions, found significantly reduced *MEF2C* mRNA levels in the two patients with truncating mutations (P6 and P7), but not in the two patients with the missense mutations (P5, P8; Fig. 5A). The latter may be explained by lack of nonsense-mediated mRNA decay in missense mutations [Belgrader and Maquat 1994; Perrin-Vidoz et al., 2002].

Mef2c homozygous knockout in mice results in embryonic lethality due to cardiovascular defects even before brain development [Li et al., 2008a]. However, conditional homozygous deletion of *Mef2c* in radial glial cells during late embryogenesis and expression of a superactive form of *Mef2c* in neurons of mice indicated an essential role in hippocampal-dependent learning and memory by suppressing the number of excitatory synapses and thus regulating basal and evoked synaptic transmission [Barbosa et al., 2008]. Furthermore, after knockout in neural progenitors, an abnormal aggregation and compaction of migrating neurons during development was observed, resulting in smaller brain size with smaller, less mature neurons in adult mice, which also showed aberrant electrophysiology and behavioral anomalies like altered anxiety and paw-clasping resembling those seen in mouse models of Rett syndrome [Li et al., 2008a].

Rett syndrome is a devastating neurological disorder classically affecting young girls and leading to rapid loss of sensory-motor capacities and autonomy. It has an estimated prevalence of 1:8,500 by age 15 years in females [Laurvick et al., 2006]. Classical Rett syndrome (MIM♯ 312750) is characterized by apparently normal psychomotor development during the first 6 to 18 months of life until a short period of developmental stagnation occurs, followed by rapid regression in language and motor skills and a long-term stability at a low functional level. During the phase of rapid
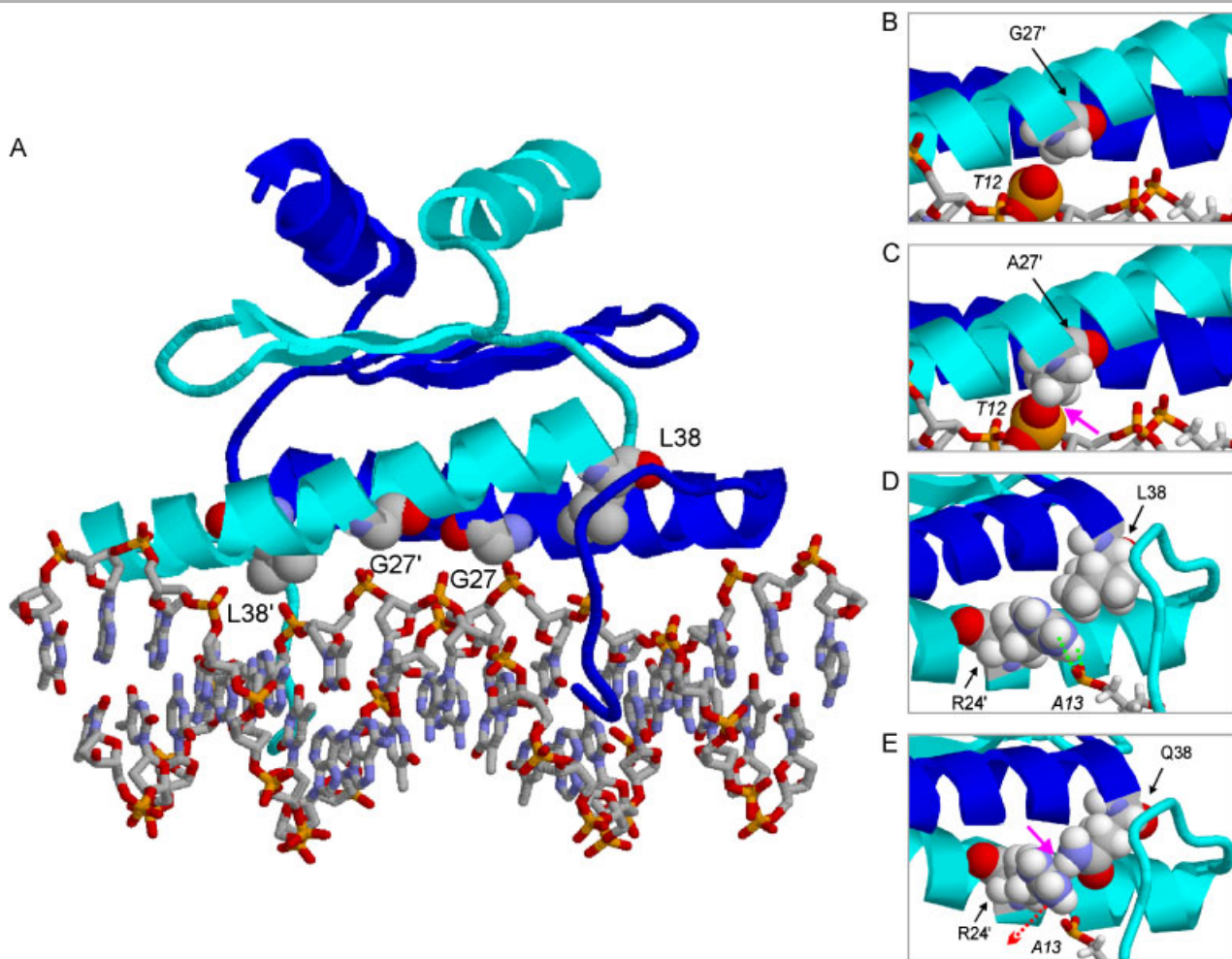
Figure 4. Effects of the mutations on the MEF2C structure and DNA binding properties. **A:** Crystal structure of the MEF2A–DNA complex. MEF2A and MEF2C only differ by a single amino acid in the DNA binding domain, thus rendering the MEF2A structure a suitable template for subsequent analysis. The two subunits of the dimeric protein are colored in blue and cyan, respectively, and the bound DNA is shown in stick presentation. The mutant residues are shown in space-filled presentation and are labeled (primes denote residues of the second subunit). The crystal structure reveals that both G27 and L38 are located close to the protein–DNA interface. **B, C:** Modeling of the effect of the G27A mutation: G27 is situated at a structurally demanding position and allows the helix of MEF2C to come close to the DNA backbone. G27 is in close proximity to the phosphate group of nucleotide T12 of the bound DNA (**B**), whereas a replacement to alanine leads to clashes with the phosphate group (panel **C**; magenta arrow). Removal of this clash will result in conformational rearrangements at the protein–DNA interface and consequently lead to weaker DNA binding. **D, E:** Modeling of the effect of the L38Q mutation: L38 does not directly interact with the DNA, but has already been reported previously to play a role for restricting the conformational flexibility of the long side chains involved in DNA binding [Santelli and Richmond, 2000]. L38 is important for the proper positioning of R24′ with respect to the DNA (panel **D**; green lines indicate the interaction of R24 with nucleotide A13). **E:** A mutation of L38 to glutamine causes steric clashes between the Q38 side chain amide with the guanidino group of R24 (magenta arrow). This will lead to a rearrangement of the R24 sidechain (red arrow), which is then no longer in an optimal position for an interaction with nucleotide A13. This effect is therefore expected to cause a decreased affinity of MEF2C for its DNA binding site. In addition, the presence of a novel functional side chain in the DNA binding site of the Q38-mutant might also affect the specificity of DNA binding.

regression, purposeful hand use is replaced by repetitive, stereotypic hand movements. Further signs are autistic features, fits of screaming and inconsolable crying, episodic apnea and/or hyperpnea, gait ataxia and apraxia, tremors, bruxism, seizures, and acquired microcephaly. Besides the classical form, several variant forms such as mental retardation with spasticity, congenital hypotonia with infantile spasms or severe neonatal encephalopathy in males have been delineated. Although in about 90% of patients with classical Rett syndrome mutations or deletions of the X-linked *MECP2* gene were detectable, less than 50% of atypical patients showed *MECP2* defects [Fukuda et al., 2005; Kammoun et al., 2004; Li et al., 2007; Zahorakova et al., 2007]. Few of the *MECP2* negative patients were recently shown to

suffer from *CDKL5* [Archer et al., 2006; Weaving et al., 2004] or *FOXG1* [Ariani et al., 2008; Mencarelli et al., 2010; Philippe et al., 2010] mutations. Most patients with 5q14.3q15 microdeletion or *MEF2C* mutation do not show classical Rett syndrome with aquired microcephaly and developmental regression after an initial normal interval, but commonly resemble Rett-like patients with congenital–hypotonia–infantile spasms variant who suffer from primary hypotonia, severe mental and motor retardation, and early onset seizures, and occasionally from autistic behavior, stereotypic hand movements, and episodic hyperventilation. However, case 7 by Le Meur et al. [2010] with a *MEF2C* stop mutation was reported to have had normal development until the age of 5 months, followed by developmental regression, and two of
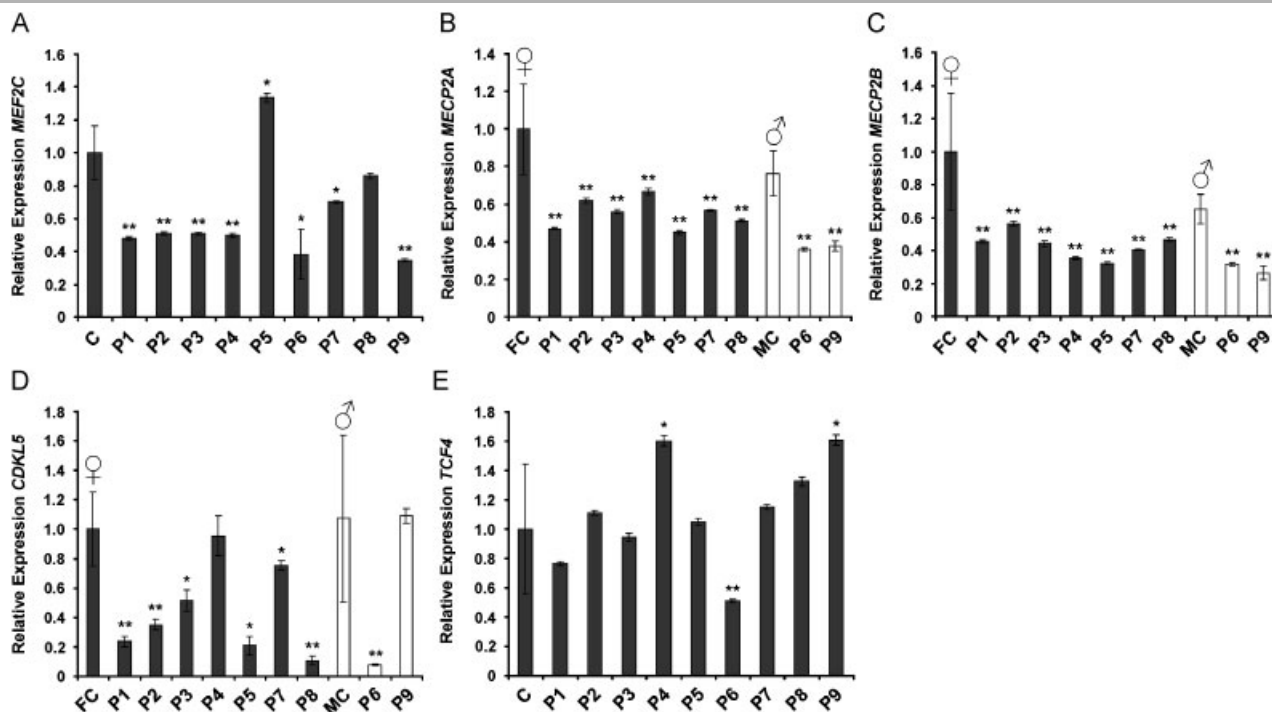
Figure 5. Expression of phenotypically related genes in patients with *MEF2C* deletions or mutations measured by quantitative real-time RT-PCR. The values of each patient were obtained in four replicates, each normalized to four different housekeeping genes, and the mean value was set in relation to the mean value of 10 controls (C), or for gender-matched controls in case of the X-linked genes *MECP2* and *CDKL5* to the values of six females (FC) or four males (MC), respectively. The diagram shows the mean values and standard deviations. *p*-values were obtained with a Wilcoxon test (*$p < 0.05$, **$p < 0.001$). **A:** *MEF2C* expression was significantly decreased in P1, P2, P3, P4, and P9, with deletions in the region of *MEF2C* and in P6 and P7 with truncating mutations in *MEF2C*, whereas it was increased or normal in P5 and P8, respectively, harboring missense mutations. **B, C:** *MECP2* expression of both isoforms was significantly decreased in all tested patients compared to gender matched controls. **D:** Expression of *CDKL5* was decreased in the majority of patients (P1, P2, P3, P5, P6, P7, and P8) but not consistently in all patients. **E:** Expression of *TCF4* was not consistently altered in patients with *MEF2C* deletions or mutations.

our patients and one patient reported by Le Meur et al. [2010] showed head circumferences around the lower border. This phenotypical overlap is in line with molecular findings indicating involvement of MECP2 and CDKL5 in a common pathway [Mari et al., 2005], and MECP2 binding to the murine *Mef2c* promoter as a repressor [Chahrour et al., 2008]. On the other hand, in muscle development MEF2 proteins and myogenic basic helix-loop-helix (bHLH) factors are known to regulate the expression of each other as well as forming dimers to cooperatively regulate gene expression of common target genes [Molkentin and Olson 1996]. Because bHLH transcription factors play a crucial role in the commitment of neural progenitor cells to a specific neural fate, interaction with MEF2C may also be important for neuronal development [Janson et al., 2001; Powell and Jarman 2008], and may explain phenotypic overlap of Rett-like disorders and Pitt-Hopkins syndrome, which is caused by haploinsufficiency of the bHLH transcription factor *TCF4* [Zweier et al., 2008].

We therefore investigated expression levels of *MECP2*, *CDKL5*, and *TCF4* in blood samples of patients with 5q14.3q15 microdeletions (P1–4, P9) or *MEF2C* mutations (P5–P8). We found expression of both *MECP2* isoforms significantly diminished in all patients, further indicating a common pathway of MEF2C and MECP2 (Fig. 5B and C). *CDKL5* expression was also commonly reduced apart from two patients with a microdeletion (P4, P9) (Fig. 5D). In contrast, *TCF4* expression levels were generally unchanged apart from patient P4 and P9 with a microdeletion, who showed increased levels and patient P6 with a *MEF2C* mutation, who showed decreased levels (Fig. 5E).

Although alterations of expression levels in blood may not necessarily represent the situation in neuronal cells, function of these neuronal genes seems to be reflected in abnormal expression patterns in peripheral blood of affected patients.

Because MEF2 proteins interact with myogenic basic helix-loop-helix transcription factors that bind to E-boxes [Black and Olson 1998], we analyzed the effect of the *MEF2C* mutations in a transcriptional reporter assay. Cotransfection of *MEF2C,* together with the 4 × EtkGL2 vector containing E-boxes and a MADS consensus binding site, significantly increased transcriptional activity indicating synergism with an unidentified endogenous transcription factor in transactivation of the luciferase reporter. Transfection with the mutated *MEF2C* constructs containing the stop mutation E34X or the missense mutation L38Q resulted in transcriptional activity levels of the endogenous factors only, indicating complete loss of MEF2C function. The mutation G27A also showed significantly decreased transcriptional activity, but to a lesser extend. Thus, we confirmed loss of function as the underlying mechanism in the observed *MEF2C* mutations.

To investigate if the constantly reduced *MECP2* expression levels in our patients with *MEF2C* deletions or mutations were caused by a transcriptional interaction, we cloned the whole promoter region (−1,071 until +9 bp) of *MECP2* [Liu and Francke 2006], which contains several E-box binding motifs, upstream of a luciferase gene into the pGL3 vector (Fig. 6B). We found a very high endogenous activity of the *MECP2* promoter, which showed a significant further increase when cotransfected with *MEF2C* wild type. All *MEF2C* mutations, the stop, and both missense
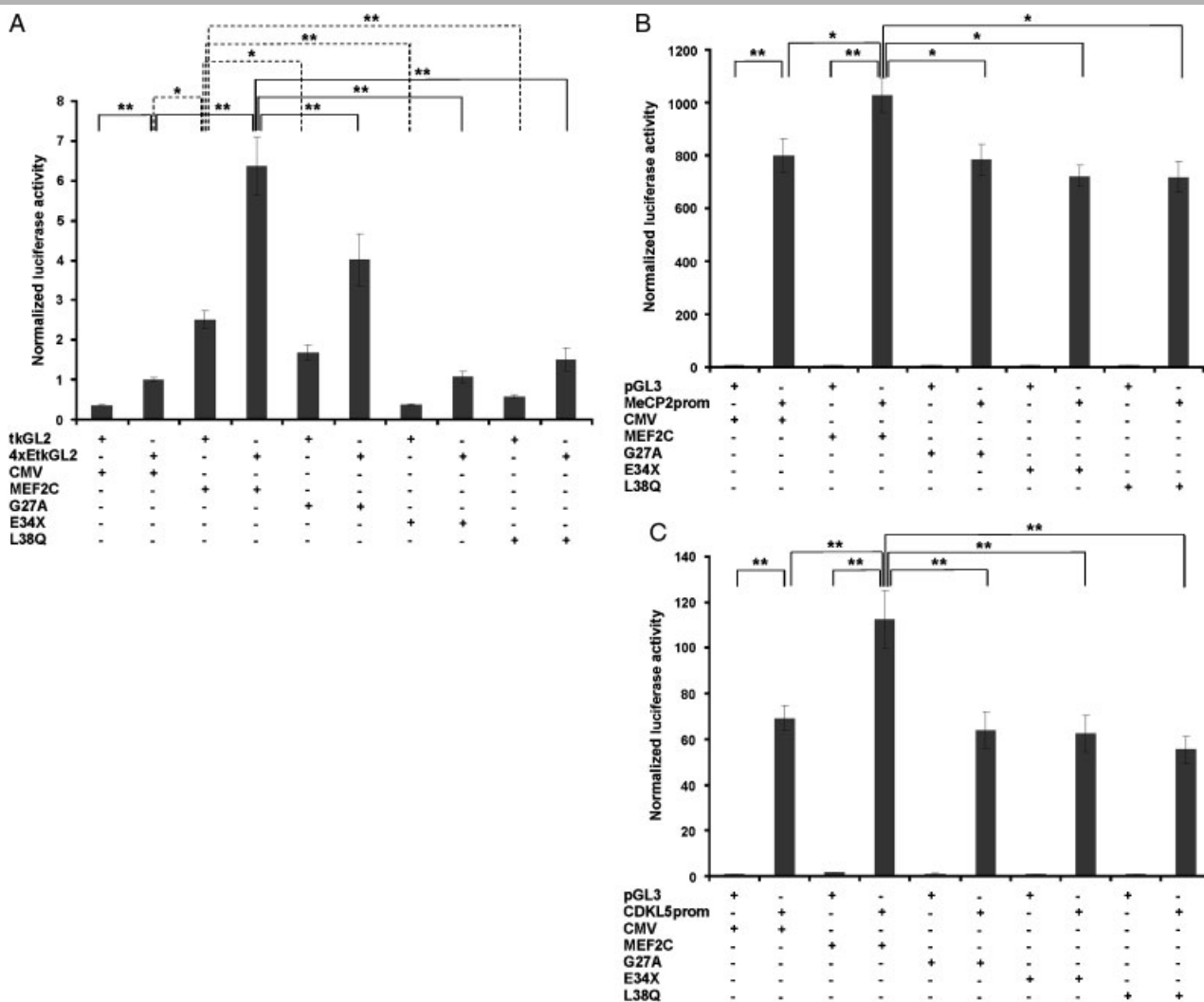
Figure 6. Wild-type *MEF2C* transcriptional activation of three different luciferase reporter constructs based on the tkGL2 or pGL3 vectors and abrogation by *MEF2C* mutations. JEG3 cells were cotransfected with one of three specific reporter constructs, respectively, and either a CMV control vector, or the *MEF2C* wild-type or mutant constructs. **A:** Cotransfection of the luciferase reporter construct containing a MADS consensus binding site and four E-boxes (4 × EtkGL2) with the *MEF2C* wild type showed a significantly increased activation when compared to either the activation resulting from endogenous transcription factors (second column) or the MEF2C activation through the MADS binding site alone (third column). All *MEF2C* mutations G27A, E34X, and L38Q showed significantly less transcriptional activity than the wild type, and the stop mutation even abolished the activation level to the endogenous background level. **B:** The luciferase reporter construct containing the promoter of *MECP2* (MECP2prom) alone showed an 800-fold increased activation of the luciferase gene compared to the empty luciferase vector (pGL3). Cotransfection of *MEF2C* showed an additional significant increase of the promoter activation. All *MEF2C* mutants abrogated the wild-type coactivation of the *MECP2* promoter. **C:** The luciferase reporter construct containing the promoter region of *CDKL5* (CDKL5prom) showed a 70-fold increased activation of the luciferase gene compared to the empty luciferase vector (pGL3). Cotransfection of *MEF2C* showed also a significant increase of the promoter activation, whereas transfection with mutants lead to abrogation of the wild-type coactivation of the *CDKL5* promoter. The *p*-values for all three experiments were obtained using the Student *t*-test, $^*p < 0.008$, $^{**}p < 0.0006$. Results depicted were obtained from experiments containing three replicates performed for each setup in parallel and shown as mean with standard deviation. Results were confirmed by a second independent experiment again with three replicates each. The *p*-values were calculated using the total of six values from the two independent experiments. Data were standardized in relation to the 4 × EtkGL2 reporter construct cotransfected with the empty CMV (**A**) or the empty pGL3 reporter contruct cotransfected with the empty CMV (**B, C**).

mutations diminished transcriptional activation of the *MECP2* promoter to the endogenous level.

Because *CDKL5* expression levels also were reduced in the majority of our patients, we also investigated the effect of wild type and mutant MEF2C on activation of the *CDKL5* promoter region, which also contains E-boxes. We observed endogenous activity of the *CDKL5* promoter region, which showed a further significant increase when cotransfected with *MEF2C* wild type (Fig. 6C). As seen in the MECP2 promoter to the *MECP2* promoter transcriptional reporter assay, the stop and both

missense mutations diminished transcriptional activation of the *CDKL5* promoter region to the endogenous level. We therefore assume a direct or indirect involvement of MEF2C in the transcriptional control of the *MECP2* and *CDKL5* genes.

In conclusion, we demonstrate that autosomal dominant de novo *MEF2C* mutations cause severe mental retardation with phenotypical overlap to Rett syndrome, which may be explained by a common pathway because patients with *MEF2C* defects showed diminished *MECP2* and *CDKL5* expression, and *MEF2C* mutations in vitro resulted in diminished transactivation of both

the *MECP2* and *CDKL5* promoters. Of note, our results suggest that expression studies in patients' blood samples may reflect affected neuronal pathways, which should encourage further similar studies that may allow novel insights in human mental retardation pathways even in the absence of suitable neuronal tissue. The high frequency of *MEF2C* mutations in ~1% of patients with severe mental retardation and ~2% of patients with Rett-like disorders underlines its importance in the differential diagnosis in such patients. Although *Mef2c* was implicated in many developmental pathways, *MEF2C* haploinsufficiency in humans apparently impairs only its central nervous function.

Acknowledgments

References

Amiel J, Rio M, de Pontual L, Redon R, Malan V, Boddaert N, Plouin P, Carter NP, Lyonnet S, Munnich A, Colleaux L. 2007. Mutations in TCF4, encoding a class I basic helix-loop-helix transcription factor, are responsible for Pitt-Hopkins syndrome, a severe epileptic encephalopathy associated with autonomic dysfunction. Am J Hum Genet 80:988–993.

Archer HL, Evans J, Edwards S, Colley J, Newbury-Ecob R, O'Callaghan F, Huyton M, O'Regan M, Tolmie J, Sampson J, Clarke A, Osborne J. 2006. CDKL5 mutations cause infantile spasms, early onset seizures, and severe mental retardation in female patients. J Med Genet 43:729–734.

Ariani F, Hayek G, Rondinella D, Artuso R, Mencarelli MA, Spanhol-Rosseto A, Pollazzon M, Buoni S, Spiga O, Ricciardi S, Meloni I, Longo I, Mari F, Broccoli V, Zappella M, Renieri A. 2008. FOXG1 is responsible for the congenital variant of Rett syndrome. Am J Hum Genet 83:89–93.

Barbosa AC, Kim MS, Ertunc M, Adachi M, Nelson ED, McAnally J, Richardson JA, Kavalali ET, Monteggia LM, Bassel-Duby R, Olson EN. 2008. MEF2C, a transcription factor that facilitates learning and memory by negative regulation of synapse numbers and function. Proc Natl Acad Sci USA 105:9391–9396.

Belgrader P, Maquat LE. 1994. Nonsense but not missense mutations can decrease the abundance of nuclear mRNA for the mouse major urinary protein, while both types of mutations can facilitate exon skipping. Mol Cell Biol 14:6326–6336.

Black BL, Olson EN. 1998. Transcriptional control of muscle development by myocyte enhancer factor-2 (MEF2) proteins. Annu Rev Cell Dev Biol 14:167–196.

Brockschmidt A, Todt U, Ryu S, Hoischen A, Landwehr C, Birnbaum S, Frenck W, Radlwimmer B, Lichter P, Engels H, Driever W, Kubisch C, Weber RG. 2007. Severe mental retardation with breathing abnormalities (Pitt-Hopkins syndrome) is caused by haploinsufficiency of the neuronal bHLH transcription factor TCF4. Hum Mol Genet 16:1488–1494.

Cardoso C, Boys A, Parrini E, Mignon-Ravix C, McMahon JM, Khantane S, Bertini E, Pallesi E, Missirian C, Zuffardi O, Novara F, Villard L, Giglio S, Chabrol B, Slater HR, Moncla A, Scheffer IE, Guerrini R. 2009. Periventricular heterotopia, mental retardation, and epilepsy associated with 5q14.3–q15 deletion. Neurology 72:784–792.

Chahrour M, Jung SY, Shaw C, Zhou X, Wong ST, Qin J, Zoghbi HY. 2008. MeCP2, a key contributor to neurological disease, activates and represses transcription. Science 320:1224–1229.

Edmondson DG, Lyons GE, Martin JF, Olson EN. 1994. Mef2 gene expression marks the cardiac and skeletal muscle lineages during mouse embryogenesis. Development 120:1251–1263.

Engels H, Wohlleber E, Zink A, Hoyer J, Ludwig KU, Brockschmidt FF, Wieczorek D, Moog U, Hellmann-Mersch B, Weber RG, Willatt L, Kreiss-Nachtsheim M, Firth HV, Rauch A. 2009. A novel microdeletion syndrome involving 5q14.3–q15: clinical and molecular cytogenetic characterization of three patients. Eur J Hum Genet 17:1592–1599.

Fukuda T, Yamashita Y, Nagamitsu S, Miyamoto K, Jin JJ, Ohmori I, Ohtsuka Y, Kuwajima K, Endo S, Iwai T, Yamagata H, Tabara Y, Miki T, Matsuishi T, Kondo I. 2005. Methyl-CpG binding protein 2 gene (MECP2) variations in Japanese patients with Rett syndrome: pathological mutations and polymorphisms. Brain Dev 27:211–217.

Hamdan FF, Gauthier J, Spiegelman D, Noreau A, Yang Y, Pellerin S, Dobrzeniecka S, Cote M, Perreault-Linck E, Carmant L, D'Anjou G, Fombonne E, Addington AM, Rapoport JL, Delisi LE, Krebs MO, Mouaffak F, Joober R, Mottron L, Drapeau P, Marineau C, Lafrenière RG, Lacaille JC, Rouleau GA, Michaud JL, Synapse to Disease Group. 2009. Mutations in SYNGAP1 in autosomal nonsyndromic mental retardation. N Engl J Med 360:599–605.

Hooft RW, Vriend G, Sander C, Abola EE. 1996. Errors in protein structures. Nature 381:272.

Janson CG, Chen Y, Li Y, Leifer D. 2001. Functional regulatory regions of human transcription factor MEF2C. Brain Res Mol Brain Res 97:70–82.

Kammoun F, de Roux N, Boespflug-Tanguy O, Vallee L, Seng R, Tardieu M, Landrieu P. 2004. Screening of MECP2 coding sequence in patients with phenotypes of decreasing likelihood for Rett syndrome: a cohort of 171 cases. J Med Genet 41:e85.

Laskowski RA, Moss DS, Thornton JM. 1993. Main-chain bond lengths and bond angles in protein structures. J Mol Biol 231:1049–1067.

Laurvick CL, de Klerk N, Bower C, Christodoulou J, Ravine D, Ellaway C, Williamson S, Leonard H. 2006. Rett syndrome in Australia: a review of the epidemiology. J Pediatr 148:347–352.

Le Meur N, Holder-Espinasse M, Jaillard S, Goldenberg A, Joriot S, Amati-Bonneau P, Guichet A, Barth M, Charollais A, Journel H, Auvin S, Boucher C, Kerckaert JP, David V, Manouvrier-Hanu S, Saugier-Veber P, Frébourg T, Dubourg C, Andrieux J, Bonneau D. 2010. MEF2C haploinsufficiency caused either by microdeletion of the 5q14.3 region or mutation is responsible for severe mental retardation with stereotypic movements, epilepsy and/or cerebral malformations. J Med Genet 47:22–29.

Leifer D, Krainc D, Yu YT, McDermott J, Breitbart RE, Heng J, Neve RL, Kosofsky B, Nadal-Ginard B, Lipton SA. 1993. MEF2C, a MADS/MEF2-family transcription factor expressed in a laminar distribution in cerebral cortex. Proc Natl Acad Sci USA 90:1546–1550.

Li H, Radford JC, Ragusa MJ, Shea KL, McKercher SR, Zaremba JD, Soussou W, Nie Z, Kang YJ, Nakanishi N, Okamoto S, Roberts AJ, Schwarz JJ, Lipton SA. 2008a. Transcription factor MEF2C influences neural stem/progenitor cell differentiation and maturation in vivo. Proc Natl Acad Sci USA 105:9397–9402.

Li MR, Pan H, Bao XH, Zhang YZ, Wu XR. 2007. MECP2 and CDKL5 gene mutation analysis in Chinese patients with Rett syndrome. J Hum Genet 52:38–47.

Li Z, McKercher SR, Cui J, Nie Z, Soussou W, Roberts AJ, Sallmen T, Lipton JH, Talantova M, Okamoto S, Lipton SA. 2008b. Myocyte enhancer factor 2C as a neurogenic and antiapoptotic transcription factor in murine embryonic stem cells. J Neurosci 28:6557–6568.

Liu J, Francke U. 2006. Identification of *cis*-regulatory elements for MECP2 expression. Hum Mol Genet 15:1769–1782.

Lyons GE, Micales BK, Schwarz J, Martin JF, Olson EN. 1995. Expression of mef2 genes in the mouse central nervous system suggests a role in neuronal maturation. J Neurosci 15:5727–5738.

Mari F, Azimonti S, Bertani I, Bolognese F, Colombo E, Caselli R, Scala E, Longo I, Grosso S, Pescucci C, Ariani F, Hayek G, Balestri P, Bergo A, Badaracco G, Zappella M, Broccoli V, Renieri A, Kilstrup-Nielsen C, Landsberger N. 2005. CDKL5 belongs to the same molecular pathway of MeCP2 and it is responsible for the early-onset seizure variant of Rett syndrome. Hum Mol Genet 14:1935–1946.

Mencarelli M, Spanhol-Rosseto A, Artuso R, Rondinella D, De Filippis R, Bahi-Buisson N, Nectoux J, Rubinsztajn R, Bienvenu T, Moncla A, Chabrol B, Villard L, Krumina Z, Armstrong J, Roche A, Pineda M, Gak E, Mari F, Ariani F, Renieri A. 2010. Novel FOXG1 mutations associated with the congenital variant of Rett syndrome. J Med Genet 47:49–53.

Molkentin JD, Olson EN. 1996. Combinatorial control of muscle development by basic helix-loop-helix and MADS-box transcription factors. Proc Natl Acad Sci USA 93:9366–9373.

Perrin-Vidoz L, Sinilnikova OM, Stoppa-Lyonnet D, Lenoir GM, Mazoyer S. 2002. The nonsense-mediated mRNA decay pathway triggers degradation of most BRCA1 mRNAs bearing premature termination codons. Hum Mol Genet 11:2805–2814.

Philippe C, Amsallem D, Francannet C, Lambert L, Saunier A, Verneau F, Jonveaux P. 2010. Phenotypic variability in Rett syndrome associated with FOXG1 mutations in females. J Med Genet 47:59–65.

Potthoff MJ, Olson EN. 2007. MEF2: a central regulator of diverse developmental programs. Development 134:4131–4140.

Powell LM, Jarman AP. 2008. Context dependence of proneural bHLH proteins. Curr Opin Genet Dev 18:411–417.

Rauch A, Thiel CT, Schindler D, Wick U, Crow YJ, Ekici AB, van Essen AJ, Goecke TO, Al-Gazali L, Chrzanowska KH, Zweier C, Brunner HG, Becker K, Curry CJ, Dallapiccola B, Devriendt K, Dörfler A, Kinning E, Megarbane A, Meinecke P, Semple RK, Spranger S, Toutain A, Trembath RC, Voss E, Wilson L, Hennekam R, de Zegher F, Dörr HG, Reis A. 2008. Mutations in the pericentrin (PCNT) gene cause primordial dwarfism. Science 319:816–819.

Santelli E, Richmond TJ. 2000. Crystal structure of MEF2A core bound to DNA at 1.5 A resolution. J Mol Biol 297:437–449.

Shore P, Sharrocks AD. 1995. The MADS-box family of transcription factors. Eur J Biochem 229:1–13.

Stehling-Sun S, Dade J, Nutt SL, DeKoter RP, Camargo FD. 2009. Regulation of lymphoid versus myeloid fate "choice" by the transcription factor Mef2c. Nat Immunol 10:289–296.

van Kogelenberg M, Ghedia S, McGillivray G, MacDermot K, Nelson J, Nagarajan L, Veltman JA, de Brouwer A, van Bokhoven H, MacKinley Gardner R, van Bokhoven H, Kirk EP, Robertson SP. 2010. Periventricular heterotopia is associated with common microdeletion syndromes. Mol Syndromol 1: 35–41.

Weaving LS, Christodoulou J, Williamson SL, Friend KL, McKenzie OL, Archer H, Evans J, Clarke A, Pelka GJ, Tam PP, Watson C, Lahooti H, Ellaway CJ, Bennetts B, Leonard H, Gécz J. 2004. Mutations of CDKL5 cause a severe neurodevelopmental disorder with infantile spasms and mental retardation. Am J Hum Genet 75:1079–1093.

Zahorakova D, Rosipal R, Hadac J, Zumrova A, Bzduch V, Misovicova N, Baxova A, Zeman J, Martasek P. 2007. Mutation analysis of the MECP2 gene in patients of Slavic origin with Rett syndrome: novel mutations and polymorphisms. J Hum Genet 52:342–348.

Zweier C, Peippo MM, Hoyer J, Sousa S, Bottani A, Clayton-Smith J, Reardon W, Saraiva J, Cabral A, Gohring I, Devriendt K, de Ravel T, Bijlsma EK, Hennekam RC, Orrico A, Cohen M, Dreweke A, Reis A, Nurnberg P, Rauch A. 2007a. Haploinsufficiency of TCF4 causes syndromal mental retardation with intermittent hyperventilation (Pitt-Hopkins syndrome). Am J Hum Genet 80:994–1001.

Zweier C, Sticht H, Aydin-Yaylagul I, Campbell CE, Rauch A. 2007b. Human TBX1 missense mutations cause gain of function resulting in the same phenotype as 22q11.2 deletions. Am J Hum Genet 80:510–517.

Zweier C, Sticht H, Bijlsma EK, Clayton-Smith J, Boonen SE, Fryer A, Greally MT, Hoffmann L, den Hollander NS, Jongmans M, Kant SG, King MD, Lynch SA, McKee S, Midro AT, Park SM, Ricotti V, Tarantino E, Wessels M, Peippo M, Rauch A. 2008. Further delineation of Pitt-Hopkins syndrome: phenotypic and genotypic description of 16 novel patients. J Med Genet 45:738–744.